



Cite this: *J. Mater. Chem. A*, 2014, **2**, 15181

N-doped ordered mesoporous carbons with improved charge storage capacity by tailoring N-dopant density with solvent-assisted synthesis

Vitor C. Almeida,^{a,b,c} Rafael Silva,^b Muharrem Acerce,^d Osvaldo Pezoti Junior,^a André L. Cazetta,^a Alessandro C. Martins,^{a,b,c} Xiaoxi Huang,^b Manish Chhowalla^d and Tewodros Asefa^{*bc}

We report a facile, nanocasting synthetic method that results in nitrogen-doped mesoporous carbons with tailorable density of N-dopants and high charge storage capacity. The key step in the synthesis of the materials is the preparation of different nitrogen-functionalized SBA-15 mesoporous silicas with tunable density of organoamine groups using a simple solvent-assisted post-grafting method, and the use of the resulting materials both as hard templates as well as N-doping agents for the carbon materials forming inside the pores of SBA-15 *via* nanocasting. Accordingly, the carbonization of common carbon sources within the organoamine-functionalized SBA-15 produces mesostructured carbons containing different densities of nitrogen dopant atoms. Specifically, a polar protic solvent (ethanol) and a non-polar solvent (toluene) are used for grafting the organoamine groups, ultimately producing two different nitrogen-doped mesoporous carbons, labelled here as N-MC-E and N-MC-T, respectively. These materials possess not only different amounts of nitrogen dopant atoms (0.6 and 2.4 atomic%, respectively) but also distinct electrochemical and charge storage properties. Nitrogen sorption measurements indicate that both materials have mesoporous structures with a high surface area (typically, $\sim 800 \text{ m}^2 \text{ g}^{-1}$) and nanometer pores with an average pore size of $\sim 5 \text{ nm}$. Electrochemical measurements at 0.5 A g^{-1} reveal that the N-MC-E and N-MC-T exhibit high capacitance (152.4 F g^{-1} and 190.2 F g^{-1} , respectively). These values are either better or comparable to some of the highest capacitance values recently reported for related materials synthesized via other methods. In addition, N-MC-E and N-MC-T retain up to 98% of their stored charges or initial capacitance after 1,000 charge–discharge cycles at a current density of 2.0 A g^{-1} . These results clearly show N-MCs' good electrochemical stability as well as potential application in energy storage.

Received 4th May 2014
Accepted 7th July 2014

DOI: 10.1039/c4ta02236j
www.rsc.org/MaterialsA

Introduction

Over the past two decades, ordered mesoporous materials have garnered a great deal of scientific as well as commercial interest due to their numerous useful properties (*e.g.*, high surface area, tunable nanometer pores and high pore volume) as well as many potential applications in areas ranging from separations to nanomedicine.¹ By taking advantage of their high surface area and nanometer pore-structures, various efficient and size-

selective catalysis and effective drug delivery of large payloads of drugs have also been demonstrated.

Among various types of mesoporous materials, ordered mesoporous carbons (OMCs) are, particularly, interesting and conducive for a range of applications because of carbon materials' many additional inherent advantages, including chemical inertness, thermal stability and electrical conductivity.² These properties are also among the main reasons for carbon-based materials to find numerous commercial applications as adsorbents, catalyst support materials, electrodes in fuel cells and supercapacitors, *etc.*³

OMCs primarily consist of a family of materials called CMK-*n* (or carbon mesostructured by KAIST), which are typically synthesized *via* a method called nanocasting using nanoporous materials such as MCM-48, SBA-1, SBA-15, and SBA-16 mesoporous silicas as hard templates.⁴ In nanocasting synthesis, the nanometer pores of the nanoporous materials are immobilized or filled in with carbon precursors such as sucrose and furfuryl alcohol. After carbonization of the carbon precursors within the

^aDepartment of Chemistry, Universidade Estadual de Maringá, Av. Colombo 5790, CEP 87020-900 – Maringá, Paraná, Brazil. Fax: +55 44 3011 4449; Tel: +55 44 3011 4500

^bDepartment of Chemistry and Chemical Biology, Rutgers, The State University of New Jersey, 610 Taylor Road, Piscataway, New Jersey 08854, USA. E-mail: tasefa@rci.rutgers.edu; Fax: +1 732 4455312; Tel: +1 848 4452970

^cDepartment of Chemical and Biochemical Engineering, Rutgers, The State University of New Jersey, 98 Brett Road, Piscataway, New Jersey 08854, USA

^dDepartment of Materials Science and Engineering, Rutgers, The State University of New Jersey, 608 Taylor Road, Piscataway, New Jersey 08854, USA

resulting nanocomposite materials, the mesoporous silica hard templates are removed by dissolution, typically using basic solution.⁵ This finally results in ordered mesoporous carbons, or CMK-*n*'s, having the negative replica of the structures of the mesoporous silica frameworks used as templates.

This synthetic approach was first demonstrated by Ryoo *et al.*,⁶ who reported the synthesis of CMK-1 by using sucrose as a carbon precursor and MCM-48 as a hard template. After this pioneering work, the synthesis of other mesoporous carbonaceous materials was also demonstrated using various mesoporous materials as templates. This includes CMK-2,^{6b} CMK-3,⁷ CMK-4,⁸ and CMK-5,⁹ which were produced using SBA-1, SBA-15, MCM-48 and SBA-15, respectively, as hard templates *via* nanocasting synthesis. CMK-3, in particular, which was synthesized using sucrose as a carbon precursor in SBA-15, is one of the most commonly studied OMC materials. As it is merely the inverse replica of SBA-15,⁷ CMK-3 possesses a hexagonally ordered mesoporous structure and a high surface area. It is worth noting here though that in nanocasting synthesis of nanostructured carbon materials, besides the structures of the hard templates, the carbon precursors can also dictate the nature of the final materials. For instance, by varying the type of carbon precursors, but keeping SBA-15 as a hard template under otherwise similar nanocasting synthetic procedure, different types of nanostructured carbon materials with amorphous or graphitic structures can be produced.¹⁰

In recent years, there has been a burgeoning research effort to find synthetic routes that allow the incorporation of heteroatoms such as boron, nitrogen and oxygen into OMC materials because substitutional doping of heteroatoms within carbon nanomaterials has been found to render the latter improved semiconducting, mechanical, electronic and electrical properties.^{11–14} Furthermore, it has been shown that the presence of heteroatoms in nanostructured carbons makes the carbon materials to exhibit improved charge-exchange properties and higher electrochemical capacitance.¹⁵ This is also why some heteroatom-doped carbon nanomaterials have emerged as more appealing materials than their un-doped counterparts for applications in energy storage, electrocatalysis and so on.^{16–19}

Nitrogen-doped OMCs, in particular, are among the most studied heteroatom-doped carbon nanomaterials. They are typically synthesized through one of the following three synthetic methods: (i) *via* nanocasting using as precursors nitrogen-containing organic substances, *i.e.*, substances that can inherently leave behind N dopant atoms in the carbon materials after carbonization;^{14,20} (ii) post-treatment of OMCs under high temperature in the presence of nitrogen containing gaseous compounds, *e.g.*, ammonia; and (iii) chemical treatment of OMCs with N-containing reactive substances such as NH₃, HCN and HNO₃.¹⁹ However, most of these methods present some disadvantages as they result in carbon nanomaterials with C–N functional groups that are unstable under various conditions¹⁹ and that can destroy the structure of the mesoporous carbons, yielding non-uniformly functionalized carbon surfaces.²¹

Herein we demonstrate a new, facile synthetic method that leads to N-functionalized OMCs that possess tunable or high

density of nitrogen dopants and high charge storage capacity. The synthesis involves functionalization of SBA-15 mesoporous silica with controlled density of surface organoamine groups through solvent-assisted grafting, using toluene or ethanol as a solvent, followed by the use of these materials as hard templates in nanocasting synthesis of carbon nanostructures. The resulting N-doped OMCs show tailorabile or high capacitance, depending on the amount of nitrogen dopant atoms in them, which is controlled by the type of solvent used to make their parent organoamine-functionalized SBA-15 materials. It is worth noting that one of the unique features of our synthesis is that the parent materials used as templates during nanocasting are also the ones that serve as nitrogen doping agents for the final N-doped OMCs (*cf.* in previous cases, either the carbon precursors themselves or other external N-containing agents used after the synthesis of the carbon materials are the sources of the nitrogen dopant atoms in the final N-doped OMCs).

Experimental section

Materials and reagents

EO₂₀–PO₇₀EO₂₀ (Pluronic P123) was purchased from BASF. Tetraethyl orthosilicate (TEOS, 98%) was obtained from Acros. 3-Aminopropyltrimethoxysilane (APTS) was purchased from Gelest, Inc. Anhydrous toluene and anhydrous ethanol were acquired from Fisher Scientific. Hydrogen peroxide (H₂O₂), sodium hydroxide (NaOH), sulfuric acid (H₂SO₄), ferric chloride (FeCl₃), sucrose, carbon black and polytetrafluoroethylene (PTFE) were purchased from Sigma-Aldrich.

Synthesis of N-doped ordered mesoporous carbons (N-MCs) by combining solvent-assisted grafting with nanocasting

To synthesize the N-doped OMCs (dubbed here as N-MCs), first mesoporous silica (SBA-15) was prepared using Pluronic P123 as a surfactant and TEOS as a silica source, by following the synthesis procedure reported by Zhao *et al.*²² The surfactant templates were removed from the as-synthesized mesostructured silica by treating the latter with H₂O₂, according to the method reported by Xu *et al.*²³ The resulting SBA-15 was then functionalized with different densities of aminopropyl groups by stirring the SBA-15 with APTS in two solvents of differing polarity, *i.e.*, ethanol and toluene, as reported by us before.²⁴ Typically, 2 g of dry SBA-15 was stirred with APTS (14.72 mmol) in 1 L of solvent (ethanol or toluene) under reflux at 80 °C for 6 h. The solution was then filtered, and the solid product was copiously washed with toluene and/or ethanol and dried in air.

The resulting amine-functionalized SBA-15 materials were impregnated with an aqueous solution of sucrose containing sulfuric acid. In a typical synthesis, 1.0 g of the amine-functionalized SBA-15 was mixed with a solution of sucrose (1.25 g), sulfuric acid (0.14 g) and distilled water (5.0 g). The mixture was placed in an oven at 100 °C for 6 h, followed by at 160 °C for 6 h. A dark brown colored material, mesoporous silica containing carbonized sucrose, was then obtained. The material was graphitized by pyrolyzing it at 450 °C for 2 h, and then at 900 °C for 3 h. The resulting mesoporous silica–carbon nanocomposite

material was then treated with 1.0 M NaOH solution (in 50 vol% ethanol/50 vol% H₂O) in an autoclave at 100 °C for 6 h. This procedure was performed twice in order to completely remove the silica template from the composite material. The dispersion was then filtered using a filter paper (Millipore, 0.45 µm), and the solid product was washed several times with ethanol and distilled water and finally dried at 100 °C for 12 h. The resulting N-doped mesoporous carbons synthesized from the two different amine-functionalized SBA-15 materials prepared using ethanol and toluene as solvents were labeled as N-MC-E and N-MC-T, respectively. As a control sample, CMK-3 mesoporous carbon,⁷ denoted here as MC, was synthesized using “un-functionalized” SBA-15 (containing no organoamine groups) as a template, under otherwise identical synthetic conditions.

Characterizations of the materials

The surface properties and surface area of the materials were characterized by N₂ adsorption–desorption measurements at 77 K using a Quantachrome Nova 1200 surface area analyzer. Using the N₂ adsorption–desorption isotherms and the Brunauer–Emmett–Teller (BET) method, the surface areas (S_{BET}) of the materials were determined. From the amount of nitrogen adsorbed at a relative pressure (p/p^0) of 0.99, the total pore volume (V_T) of the material was obtained.²⁵ The materials' micropore volumes (V_μ) were determined by applying the Dubinin–Radushkevich equation,²⁵ and their mesopore volumes (V_m) were calculated from the difference between V_T and V_μ . The pore diameter (D_m) was calculated using the ratio of $4V_\mu/S_{\text{BET}}$, and pore distribution was obtained using the BJH method.²⁶ Transmission electron microscope (TEM) images were taken with an FEI Tecnai T-12 TEM instrument. The morphology of OMCs was examined by obtaining scanning electronic microscope (SEM) images for them with a Shimadzu SS 550 SEM instrument. FT-Raman spectra were recorded using a Horiba John-Yvon Micro Raman Spectrometer, equipped with a microscope having a 472.98 nm laser as the source of its excitation beam. FT-IR spectra were recorded between 4000 and 400 cm⁻¹ (with a resolution of 4 cm⁻¹ and an acquisition rate of 20 scan min⁻¹) using a Bomem Easy MB-100 spectrometer. Samples for FT-IR spectroscopy were prepared in solid form by mixing the N-MC materials with KBr and pressing the mixture into pellets. X-ray photoelectron spectroscopy (XPS) experiments were performed using a Kratos Axis Ultra Spectrometer that is equipped with a monochromic Al K α (1486.7 eV) beam and that is working with a voltage of 15 kV and an emission current of 10 mA.

Electrochemical and charge–discharge measurements

Electrochemical cyclic voltammetry (CV) and galvanostatic charge–discharge studies of the N-MC materials were performed with a Solartron 1480 Multistat using 6.0 M KOH solution as an electrolyte. The electrochemical cells consisted of three electrodes in which the N-MCs or the corresponding reference material were assembled to be part of the working electrode (see below) and a Pt wire and a Hg/HgO electrode were used as the counter and reference electrodes, respectively. To

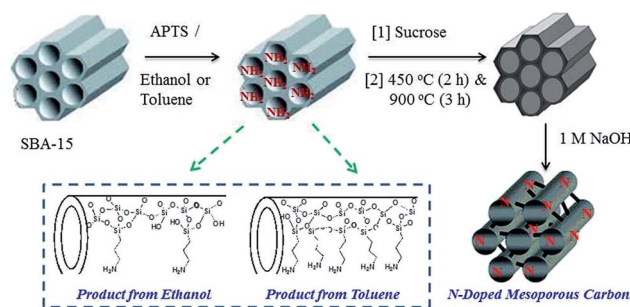
prepare the working electrode, the mesoporous carbon samples (85 wt%), commercially available carbon black (10 wt%) and polytetrafluoroethylene (5 wt%) in water were mixed together to form a paste, and the paste was then brushed on nickel foam having an area of 1 cm² with an active material of 7.0 mg cm⁻².

Results and discussion

Synthesis and characterization of N-MCs

The synthesis of N-doped OMCs (N-MCs) is achieved via the nanocasting method using organoamine-modified mesoporous silicas, prepared by solvent-assisted grafting, as hard templates (Scheme 1). Specifically, two different organoamine-grafted SBA-15 materials were prepared by using ethanol or toluene as a solvent. We chose these two solvents because they are shown to result in different densities and distributions of organoamine groups on the surfaces of mesoporous silica.²⁴ Besides their function as templates, the resulting organoamine-grafted SBA-15 materials with different organoamine groups were used to serve as the source of N dopant atoms onto the surfaces of the mesoporous carbons forming from carbon precursors during carbonization. We expected that the variation (or increased density) of grafted organoamine groups on the template materials can result in N-doped MCs with controlled or higher density of N-dopant atoms and distinct/improved properties (*vide infra*). Moreover, since the organoamines are predominantly on the channel walls of the host material, they were expected to end up as dopant atoms mainly on the surfaces of the mesoporous carbons. And, since the heteroatoms of heteroatom-doped carbon nanomaterials dictate many of the properties of such materials, having the heteroatoms mainly on the surfaces (or accessible locations) of the carbon materials might allow the latter to display better properties than if the dopant atoms are within the bulk of the materials.

By combining the nanocasting synthetic method with solvent-assisted grafting, two different N-doped OMCs (N-MCs) with different densities of N dopants were then synthesized. Their N₂ sorption isotherms and pore size distributions, along with the ones for their corresponding control material (MC), are depicted in Fig. 1. The results show that both N-MCs and MC



Scheme 1 Schematic illustration of the synthesis of N-doped mesoporous carbons with different amounts of N-dopants by using organoamine-grafted SBA-15 mesoporous silica materials, prepared via solvent-assisted grafting in ethanol or toluene, as templates as well as N-doping agents.

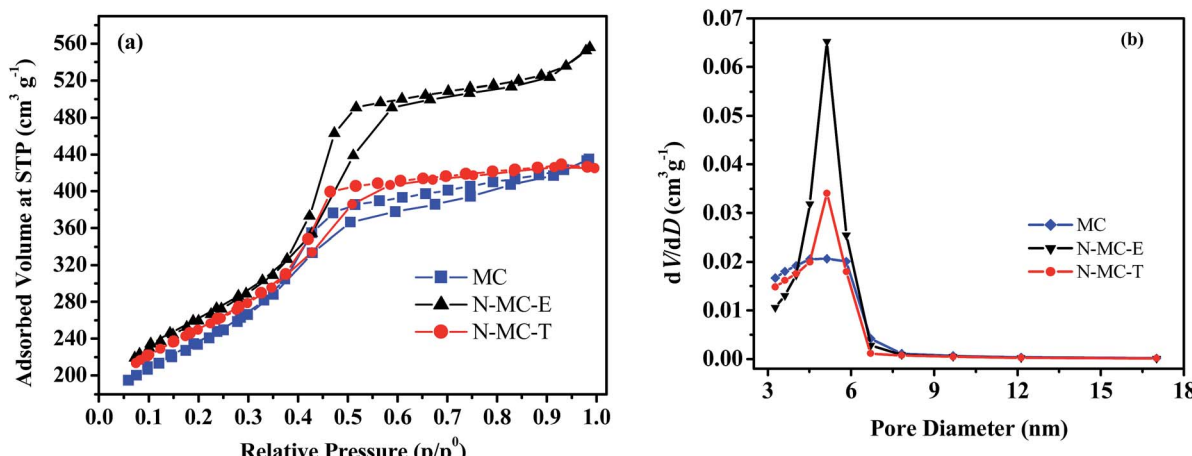


Fig. 1 N₂ adsorption–desorption isotherms (a) and pore size distributions of OMCs (b).

have Type IV isotherms, with hysteresis and capillary condensation steps at relative pressure between *ca.* 0.55–0.75, which are characteristic of mesoporous materials.²⁰

The pore size distributions of the materials indicate that the pore diameters of N-MCs are closely distributed around 5 nm. The textural properties derived from the N₂ adsorption data are shown in Table 1, and the results reveal that the surface areas (S_{BET}) of MC, N-MC-E and N-MC-T are 824, 790 and 749 m² g⁻¹, respectively. Furthermore, in all the cases, the percentage of mesopore volume is found to be >85% and their average pore diameters are found to be *ca.* 5 nm.

The TEM images of N-MCs (Fig. 2) show hexagonally ordered cylindrical mesopores that appear to be the negative replica of the structures of SBA-15. The SEM images of OMCs presented in Fig. 3a–c show rod-like particles, akin to the characteristics shapes of the SBA-15 mesoporous silica particles that were used as templates.^{27,28}

The N-MC materials were further characterized by Raman spectroscopy. In the Raman spectra of the materials (Fig. 4), peaks at *ca.* 1350 and 1600 cm⁻¹ corresponding to the characteristic D and G bands of graphitic carbons, respectively, are seen.²⁹ While the G band is indicative of the presence of a typical graphitic structure in the materials, the D band reveals the presence of edges, disordered graphene sheets, and/or amorphous carbon structures within the materials.³⁰

The compositions of the N-OMCs were further analyzed by FT-IR spectroscopy. The FT-IR spectra of MC, N-MC-E and N-MC-T (Fig. 5) reveal bands that are commonly seen in

nanostructured carbon materials.³¹ The bands at *ca.* 3429 cm⁻¹ and 1080 cm⁻¹ are attributed to the O–H and C–OH stretching bands, respectively, of phenolic groups in the materials.³² The broad band between *ca.* 1450–1700 cm⁻¹ is assigned to the symmetric stretching vibrations of pyrone and carboxylic groups³³ and the axial deformations of C–C bonds of aromatic rings in the materials.³⁴ The peaks at *ca.* 1190 cm⁻¹ and *ca.* 1115 cm⁻¹ are attributed to C–O stretching bands;³⁵ the possible minor contribution due to the Si–O bond stretching of residual SBA-15, which can also show up around this region,³⁶ is ruled out as no Si signals are observed on the XPS spectra (see below).

When comparing the spectrum of N-MC-E or N-MC-T *vis-à-vis* the corresponding spectrum of MC (Fig. 5), significant differences in the relative intensities of the signals at *ca.* 3500 cm⁻¹ as well as those at *ca.* 1600 cm⁻¹ can be observed. This difference in signal intensity can be correlated with the presence or absence of N species and their density in the materials, as also confirmed by XPS analyses. For example, the signal at *ca.* 3400 cm⁻¹, which can be assigned to N–H bond stretching and/or O–H bond vibration,¹³ is higher in the FTIR spectrum of N-MC-E than that of MC or N-MC-T. Similarly, the peak at *ca.* 1600 cm⁻¹, which can be attributed to N–H bending vibration and C–N stretching,¹³ is higher in intensity in the spectrum of N-MC-T than that of MC or N-MC-E. These results seem to suggest that compared with MC both N-MC-E and N-MCT contain a higher density of functional groups consisting of nitrogen- and oxygen-based species.

Table 1 Textural characteristics of OMCs^a

Samples	S_{BET} (m ² g ⁻¹)	V_T (cm ³ g ⁻¹)	V_μ (cm ³ g ⁻¹)	V_m (cm ³ g ⁻¹)	V_m/V_T (%)	D_p (nm)
MC	824	0.673	0.067	0.606	90.0	5.14
N-MC-E	790	0.860	0.091	0.769	89.4	5.12
N-MC-T	749	0.657	0.097	0.560	85.2	5.14

^a S_{BET} = BET surface area, V_T = total pore volume, V_μ = micropore volume, V_m = mesopore volume, V_m/V_T = percentage of mesopore volume, D_p = average pore diameter (nm).

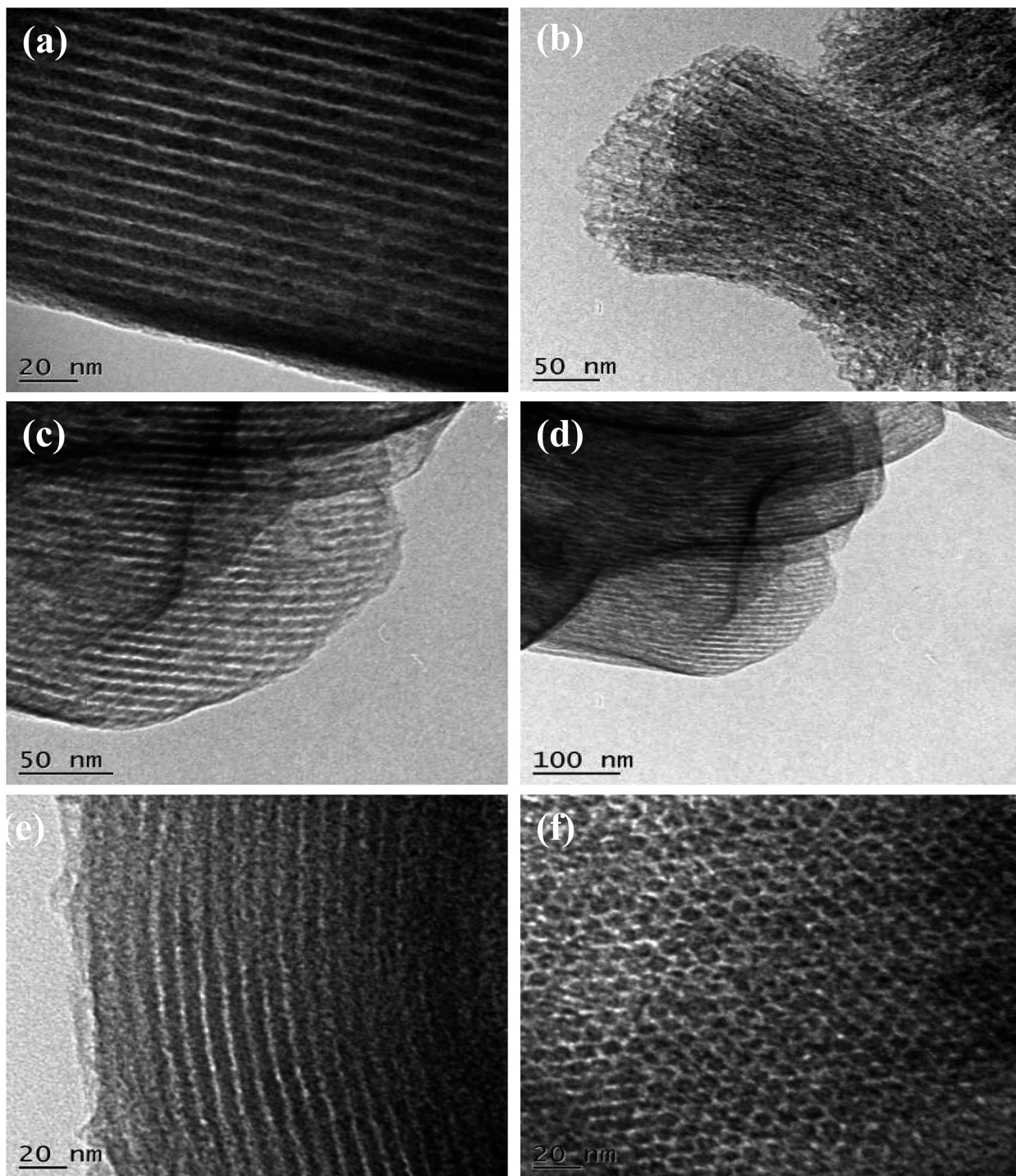


Fig. 2 TEM images of N-MCs and MC. (a and b) MC; (c and d) N-MC-E; and (e and f): N-MC-T.

XPS was also used to analyze the elemental composition of the N-MCs. Fig. 6 shows the XPS spectra of MC, N-MC-E and N-MC-T. The results indicate that whereas the MC consists of carbon and oxygen atoms, the N-MC-E and N-MC-T contain a substantial amount of nitrogen atoms besides carbon and oxygen. This is consistent with the results obtained from FTIR spectra. The presence of oxygen in the materials is not unprecedented, considering the fact that oxygenated

functional groups are quite commonly observed in carbon-based materials. In our case, the oxygen dopant may have originated from the stable residual oxygen atoms of the precursor¹¹ and/or the SBA-15 template,^{36,37} and they make their way into the carbon material aided by the high temperature employed for carbonization. The XPS spectra of the N-MCs show no silicon signals, indicating that the silica template is completely dissolved upon treatment of the

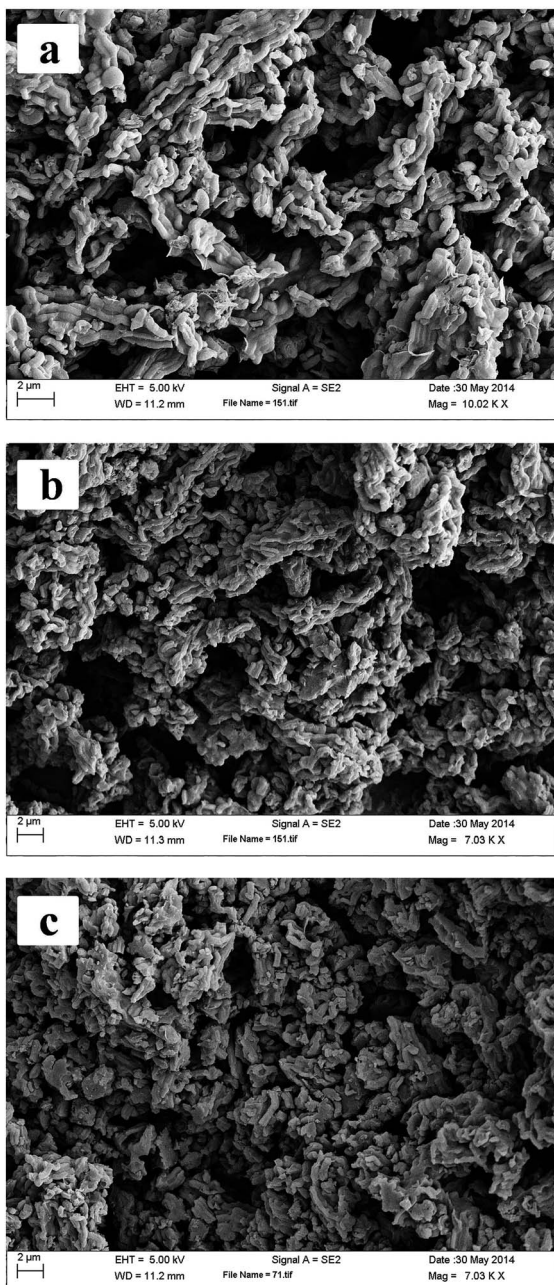


Fig. 3 SEM images of the N-MCs and MC. (A) MC; (b) N-MC-E; and (c) N-MC-T.

carbon/mesoporous silica composite materials with aqueous NaOH solution.

In Table 2, the elemental composition data of the materials, as obtained from XPS analyses, are compiled. The results further indicate that while there is no detectable nitrogen species in MC, there is a significant amount of nitrogen both in N-MC-E and in N-MC-T materials. Moreover, the data show that there is four times more nitrogen (2.4%) in N-MC-T than that in N-MC-E (0.6%), which means the solvent used for post-grafting of organoamines on the SBA-15 plays indirect but important roles in the amount of nitrogen dopant atoms incorporated into the mesoporous carbons. It is worth noting that the amount of

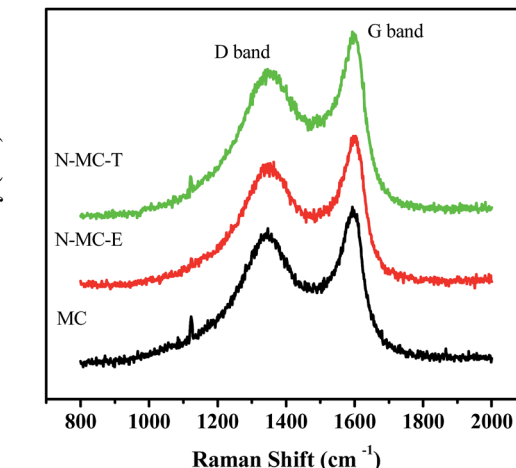


Fig. 4 Raman spectra of N-MC-E, N-MC-T and MC materials.

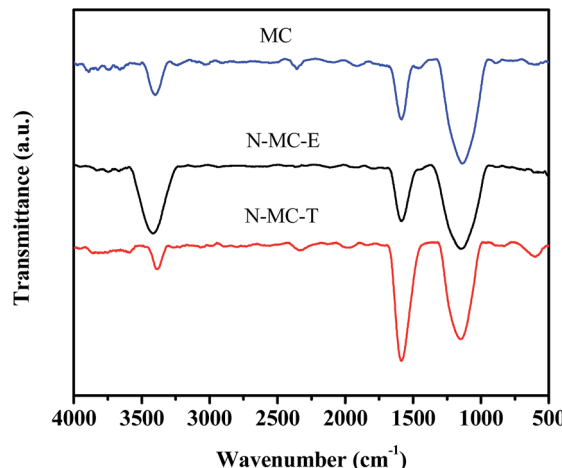


Fig. 5 FT-IR spectra of N-MC-E, N-MC-T and MC materials.

nitrogen obtained for N-MC-T in our case is quite similar to the value reported for a nitrogen-doped CMK-3, which was synthesized by post-synthetic treatment of pre-made mesoporous carbon (CMK-3) with ammonia gas.³⁸

Not surprisingly, the highest amount of nitrogen dopant atoms was obtained in the material where the organoamine groups are grafted using toluene. This result is in line with the fact that toluene results in a higher density of organoamine grafted groups (or 3.82% nitrogen) within the SBA-15 than ethanol does (which gives 1.71% nitrogen). Fig. 6b and c show the N1s XPS spectra and deconvoluted N1s peaks for N-MC-E and N-MC-T, *i.e.*, the mesoporous carbons obtained from organoamine-grafted SBA-15 prepared using ethanol and toluene as solvents, respectively. The results indicate that nitrogen species in the N-MCs exist in one of the three different forms: pyridinic (which corresponds to the peak at *ca.* 398 eV); pyrrolic/pyridone (which corresponds to the peak at *ca.* 400.38 eV) and quaternary (which corresponds to the peak at *ca.* 401.2 eV). The peak at *ca.* 398 eV is attributed to sp^2 N atoms bonded to carbon (or pyridine-like N atoms incorporated within the

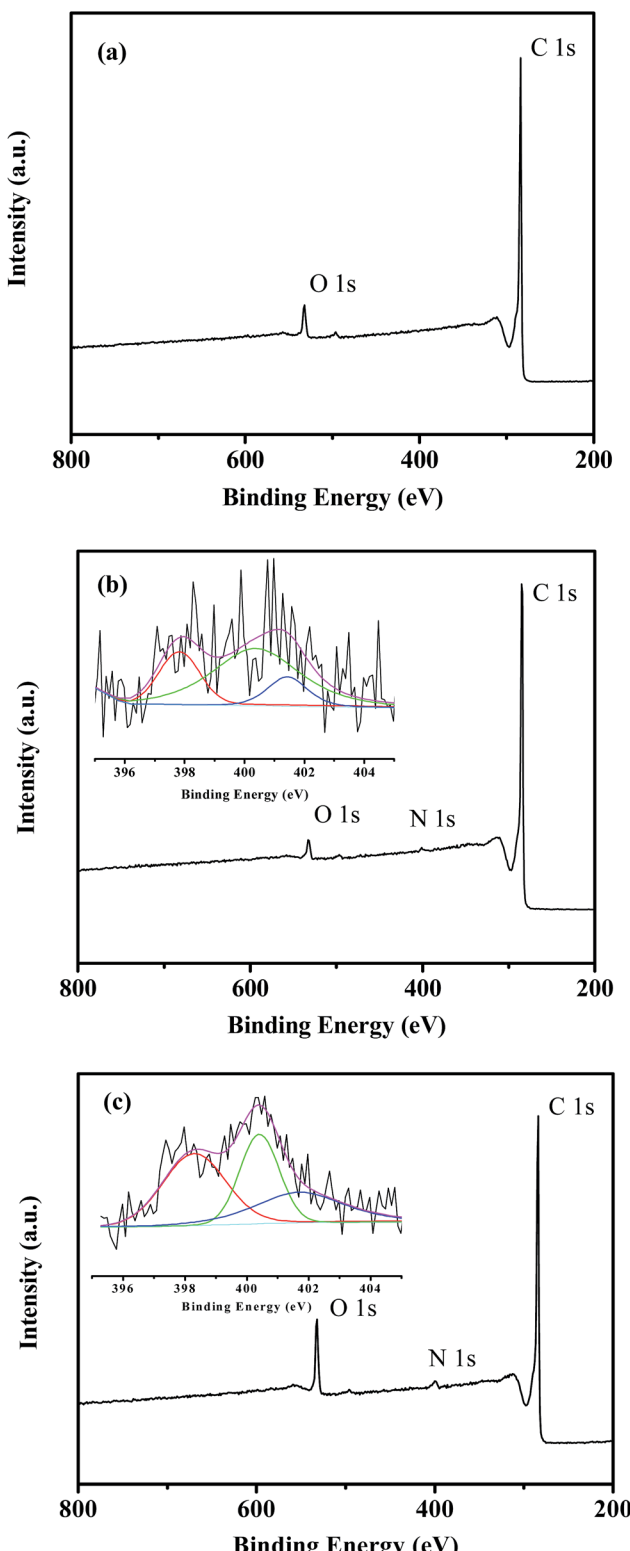


Fig. 6 XPS survey spectra and N 1s XPS spectra for MC (a), N-MC-E (b) and N-MC-T (c).

graphitic layers), whereas the peak at *ca.* 400.4 eV is assigned to nitrile groups bonded to carbon atoms of the material.¹³ The peak at *ca.* 401.6 eV is attributed to N atoms in graphite-like

Table 2 Elemental composition of MC, N-MC-E and N-MC-T determined from XPS analyses

Elements	MC (%)	N-MC-E (%)	N-MC-T (%)
C	95.2	96.6	89.4
O	4.8	2.9	8.3
N	—	0.6	2.4

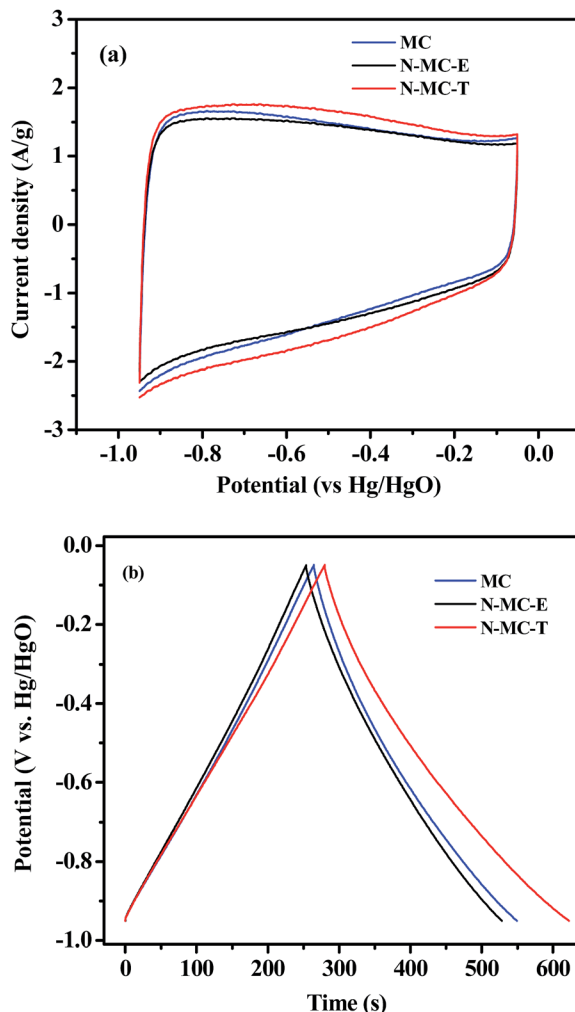


Fig. 7 (a) Cyclic voltammograms (CVs) of N-MCs and MC at a scan rate of 10 mV s⁻¹ and (b) charge–discharge curves of N-MCs and MC at a current density of 0.5 A g⁻¹.

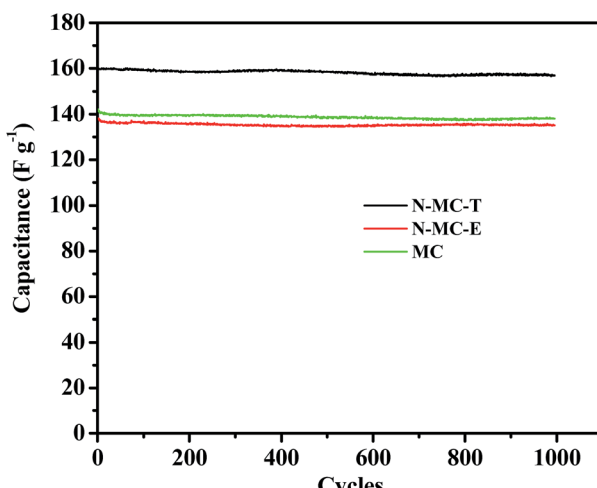
structures.³⁹ These results clearly indicate that the N-MC materials contain significant proportions of pyrrolic, quaternary nitrogen and pyridine species.

Capacitive properties of OMCs

As pyrrolic, quaternary, and pyridine nitrogen moieties in nanostructured carbon materials can impart hydrophilicity, wettability and pseudo-capacitance to the materials,¹⁴ carbon materials with significant proportions of such groups can be

Table 3 Specific capacitance (F g^{-1}) of N-MCs and MC at current densities of 0.5, 1.0, 2.0, 4.0, 8.0 and 16 A g^{-1}

Samples	Specific capacitance (F g^{-1})					
	0.5 A g^{-1}	1.0 A g^{-1}	2.0 A g^{-1}	4.0 A g^{-1}	8.0 A g^{-1}	16 A g^{-1}
MC	158.2	148.1	139.8	132.0	123.7	106.7
N-MC-E	152.4	143.8	137.1	129.3	120.9	106.7
N-MC-T	190.2	171.9	160.2	150.7	138.7	124.4

Fig. 8 Specific capacitances of MC, N-MC-E and N-MC-T as a function of cycle number (current density of 2.0 A g^{-1}).

conducive for application as electrical double-layer capacitors. It is with this anticipation that we have thus studied the electrochemical capacitive behaviors of the N-MCs we synthesized. To do this, we obtained their cyclic voltammograms (CVs) in the potential interval between -0.95 and -0.05 V (vs. Hg/HgO) at a scan rate of 10 mV s^{-1} and their galvanostatic charge–discharge profiles at a current density of 0.5 A g^{-1} . Fig. 7a shows the CVs of the electrodes containing N-MCs. All the CV curves appear to be almost rectangular-shaped, suggesting the existence of double-layer capacitance in the materials. Furthermore, the CV results indicate that N-MC-T gives the highest integrated area or specific capacitance. This is presumably due to N-MC-T's higher amount of nitrogen, consistent with a previous report,⁴⁰ where similar observations were made, or carbon nanomaterials containing nitrogen dopants were shown to have higher capacitance.

The galvanostatic charge–discharge curves of the N-MCs (Fig. 7b) appear to have a good inverse proportional size and triangular shape, which indicate that the materials have good charge storage capacity through double layer capacitance. The specific capacitance values of the N-MCs calculated from the charge–discharge curves are compiled in Table 3. The results indicate the specific capacitance of MC, N-MC-E and N-MC-T to be 158.2 , 152.4 and 190.2 F g^{-1} at 0.5 A g^{-1} . These values are very comparable or equivalent to some of the best capacitance values recently reported for related systems synthesized by other methods.^{40a,41} Furthermore, the results once again show

that N-MC-T has the highest specific capacitance among the materials we synthesized and investigated here, proving further that N dopants on carbon nanomaterials improve the materials' electrochemical capacitance. On the other hand, although the control sample, MC, does not possess nitrogen atoms, its specific capacitance is almost similar to that of N-MC-E. This is most likely due to MC's highest surface area compared to the other two materials (please note that the specific capacitance of a material is directly dependent on the material's surface area). Moreover, the presence of oxygen dopant atoms on MC's surfaces, whose amount is equivalent to the sum of nitrogen and oxygen atoms in the N-MC-E (Table 2).

Like nitrogen dopants, oxygen dopant atoms are also active in electronically promoting the pseudocapacitance of carbon nanomaterials,¹¹ albeit to a slightly lesser degree. Besides improving pseudocapacitance, the presence of nitrogen and/or oxygen species (or heteroatoms, in general) on the surfaces of the carbon materials increases the materials' hydrophilic or polar sites and wettability by electrolytes, and thereby electrical conductivity.^{41,42} Thus, overall, the presence of largest density nitrogen dopant atoms, plus some oxygen species, in N-MC-T, as characterized by XPS and FT-IR analyses, accounts for N-MC-T's highest value of specific capacitance.

The performance of N-MC materials for charge storage was then evaluated by comparing their specific capacitance at different current densities (Table 3). The results show that their specific capacitance decreases slowly as their corresponding current density increases, thus implying the materials' ability of quick charge propagation of both the double layer capacitance and pseudo-capacitance.¹¹ Additionally, as can be seen in Table 3, the N-MC materials give relatively high specific capacitance, even at a current density of 8.0 A g^{-1} , and they retain about 78, 79 and 73% of the initial capacitance when the current density is raised from 0.5 A g^{-1} to 8.0 A g^{-1} in the case of MC, N-MC-E and N-MC-T, respectively.

The electrochemical stability of N-MCs was evaluated by carrying out multiple galvanostatic charge–discharge cycles at a current density of 2.0 A g^{-1} (Fig. 8). After 1000 cycles, the materials do not display any observable loss of capacitance, thus confirming their good durability and electrochemical stability.

Conclusion

In summary, we have described the synthesis of nitrogen-doped CMK-3 type ordered mesoporous carbons (N-MCs) with tunable amount of nitrogen dopant atoms and tailorabile and efficient

capacitive charge storage properties. The materials are synthesized by first making organoamine-functionalized SBA-15 materials with solvent-assisted grafting, followed by carbonization of sucrose in the channel pores of the resulting materials, and finally etching the mesoporous silica framework with aqueous basic solution. The nitrogen dopant atoms incorporated into the mesoporous carbon are found to be dependent on the type of solvent used for grafting of the organoamine groups onto the SBA-15 material. The amounts of nitrogen incorporated into the resulting mesoporous carbons are found to be 0.6 wt% and 2.4 wt% for N-MC-E and N-MC-T, respectively, *i.e.*, the N-MCs synthesized using ethanol and toluene, respectively, as solvents for grafting the organoamine groups onto their parent materials. Moreover, the N-MCs are found to contain pyridinic, pyrrolic and quaternary nitrogen species. The specific capacitance of the N-MC-T material is determined to be higher than that of N-MC-E or MC. N-MC-T shows a specific capacitance of 190.2 F g^{-1} and retains 73% of its capacitance when the current density is increased from 0.5 A g^{-1} to 8.0 A g^{-1} . The capacitance of this material is either better or very comparable to some of the best capacitance values recently reported for related systems synthesized by other methods.^{2b,40a,41} Moreover, the materials show good stability without loss of capacitance after 1000 galvanostatic charge-discharge cycles. The reported facile synthetic strategy, combining solvent-assisted grafting with nanocasting, is shown to clearly result in OMC materials with reasonable amount of nitrogen dopant atoms, high surface area and improved capacitive charge storage properties.

Acknowledgements

VCA, OPJ and ALC acknowledge CAPEs for the financial support. TA gratefully acknowledges the financial assistance of NSF (through NSF DMR-0968937, NSF CBET-1134289, NSF ACIF, and NSF Special Creativity grant).

Notes and references

- (a) A. Walcarius and L. Mercier, *J. Mater. Chem.*, 2010, **20**, 4478; (b) R. H. Goncalves, B. H. R. Lima and E. R. Leite, *J. Am. Chem. Soc.*, 2011, **133**, 6012; (c) X. Chen and M. Antonietti, *Chem. Mater.*, 2009, **21**, 4093; (d) A. H. Lu, W. Shmidt, N. Matoussevitch, H. Bonnemann, B. Spliehoff, B. Tesche, E. Bill, W. Kiefer and F. Schüth, *Angew. Chem., Int. Ed.*, 2004, **43**, 4303; (e) G. Xu, B. Ding, P. Nie, L. Shen, H. Dou and X. Zhang, *ACS Appl. Mater. Interfaces*, 2014, **6**, 194.
- (a) T. P. Fellinger, F. Hasché, P. Strasser and M. Antonietti, *J. Am. Chem. Soc.*, 2012, **134**, 4072; (b) K. E. Shopsowitz, W. Y. Hamad and M. J. MacLachlan, *Angew. Chem., Int. Ed.*, 2011, **50**, 10991; (c) A. Walcarius, *Chem. Soc. Rev.*, 2013, **42**, 4098; (d) F. Qu, R. Nasraoui, M. Etienne, Y. Bon Saint Côme, A. Kuhn, J. Lenz, J. Gadjezik, R. Hempelmann and A. Walcarius, *Electrochim. Commun.*, 2011, **13**, 138; (e) Y. P. Zhai, Y. Q. Dou, D. Y. Zhao, P. F. Fulvio, R. T. Mayes and S. Dai, *Adv. Mater.*, 2011, **23**, 4828; (f) V. K. Saini, M. Andrade, M. L. Pinto, A. P. Carvalho and J. Pires, *Sep. Purif. Technol.*, 2010, **75**, 366; (g) B.-K. Guo, X.-Q. Wang, P. F. Fulvio, M.-F. Chi, S. M. Mahurin, X.-G. Sun and S. Dai, *Adv. Mater.*, 2011, **23**, 4661.
- (a) Z. Wu and D. Zhao, *Chem. Commun.*, 2011, **47**, 3332; (b) J. Y. Cheon, C. Ahn, D. J. You, C. Pak, S. H. Hur, J. Kim and S. H. Joo, *J. Mater. Chem. A*, 2013, **1**, 1270; (c) M. L. Lin, M.-Y. Lo and C.-Y. Mou, *J. Phys. Chem. C*, 2009, **113**, 16158; (d) C. Liu, M. Chen, C. Du, J. Zhang, G. Yin, P. Shi and Y. Sun, *Int. J. Electrochem. Sci.*, 2012, **7**, 10592; (e) D.-D. Zhou, W.-Y. Li, X.-L. Dong, Y.-G. Wang, C.-X. Wang and Y.-Y. Xia, *J. Mater. Chem. A*, 2013, **1**, 8488.
- (a) H. Yang and D. Zhao, *J. Mater. Chem.*, 2005, **15**, 1217; (b) C. Liang, Z. Li and S. Dai, *Angew. Chem., Int. Ed.*, 2008, **47**, 3696.
- (a) A. H. Lu and F. Schüth, *Adv. Mater.*, 2006, **18**, 1793; (b) Y. Fang, D. Gu, Y. Zou, Z. Wu, F. Li, R. Che, Y. Deng, B. Tu and D. Zhao, *Angew. Chem., Int. Ed.*, 2010, **49**, 7987; (c) S. B. Yoon, G. S. Chai, S. K. Kang, J. S. Yu, K. P. Gierszal and M. Jaroniec, *J. Am. Chem. Soc.*, 2005, **127**, 4188.
- (a) R. Ryoo, S. H. Joo and S. Jun, *J. Phys. Chem. B*, 1999, **103**, 7743; (b) S. H. Joo, S. J. Choi, I. Oh, J. Kwak, Z. Liu, O. Terasaki and R. Ryoo, *Nature*, 2001, **412**, 169.
- S. Jun, S. H. Joo, R. Ryoo, M. Kuk, M. Jaroniec, Z. Liu, T. Ohsuna and O. Terasaki, *J. Am. Chem. Soc.*, 2000, **122**, 10712.
- M. Kaneda, T. Tsubakiyama, A. Carlsoon, Y. Sakamoto, T. Ohsuma and O. Terasaki, *J. Phys. Chem. B*, 2002, **106**, 1256.
- A. H. Lu, W. C. Li, W. Shmidt, W. Kiefer and F. Schüth, *Carbon*, 2004, **42**, 2939.
- (a) P. F. Fulvio, P. C. Hillesheim, Y. Oyola, S. M. Mahurin, G. M. Veith and S. Dai, *Chem. Commun.*, 2013, **49**, 7289; (b) R. J. Kalbasi and N. Mosaddegh, *Mater. Chem. Phys.*, 2011, **130**, 1287; (c) T. Asefa, *Angew. Chem., Int. Ed.*, 2012, **51**, 2008.
- B. Xu, D. Zheng, M. Jia, G. Cao and Y. Yang, *Electrochim. Acta*, 2013, **98**, 176.
- Z. Lei, D. Bai and X. S. Zhao, *Microporous Mesoporous Mater.*, 2012, **147**, 86.
- N. Liu, L. Yin, C. Wang, L. Zhang, N. Lun, D. Xiang, Y. Qi and R. Gao, *Carbon*, 2010, **48**, 3579.
- X. Kim, M. Y. Kang, J. B. Joo, N. D. Kim, I. K. Song, P. Kim, J. R. Yoon and J. Yi, *J. Power Sources*, 2010, **195**, 2125.
- N. D. Kim, W. Kim, J. B. Joo, S. Oh, P. Kim, Y. Kim and J. Yi, *J. Power Sources*, 2008, **180**, 671.
- C. C. Huang, Y. H. Li, Y. W. Wang and C. H. Chen, *Int. J. Hydrogen Energy*, 2013, **38**, 3994.
- J. Tang, T. Wang, X. Sun, Y. Guo, H. Xue, H. Guo, M. Liu, X. Zhang and J. He, *Microporous Mesoporous Mater.*, 2013, **177**, 105.
- Y. Shao, X. Wang, M. Engelhard, C. Wang, S. Dai, J. Liu, Z. Yang and Y. Lin, *J. Power Sources*, 2010, **195**, 4375.
- S. H. Liu and J. R. Wu, *Int. J. Hydrogen Energy*, 2011, **36**, 87.
- Y. Xun, Z. Shu-Ping, X. We, C. Hong-You, D. Xiao-Dong, L. Xin-Mei and Y. Zi-Feng, *J. Colloid Interface Sci.*, 2007, **310**, 83.
- M. J. Lázaro, L. Calvillo, E. G. Bordejé, R. Moliner, R. Juan and C. R. Ruiz, *Microporous Mesoporous Mater.*, 2007, **103**, 158.
- D. Zhao, J. Feng, Q. Huo, N. Melosh, G. H. Fredrickson, B. F. Chmelka and G. D. Stucky, *Science*, 1998, **289**, 548.

- 23 J. Xu, M. Chen, Y. M. Liu, Y. Cao, H. Y. He and K. N. Fan, *Microporous Mesoporous Mater.*, 2009, **118**, 354.
- 24 K. K. Sharma, A. Anan, R. P. Buckley, W. Ouellette and T. Asefa, *J. Am. Chem. Soc.*, 2008, **130**, 218.
- 25 K. S. W. Sing, D. H. Everett, R. A. W. Haul, L. Moscou, R. A. Pierotti, J. Rouquerol and T. Siemieniewska, *Pure Appl. Chem.*, 1985, **57**, 603.
- 26 A. H. Basta, V. Fierro, H. El-Saied and A. Celzard, *Bioresour. Technol.*, 2009, **100**, 3941.
- 27 L. Hu, S. Dang, X. Yang and J. Dai, *Microporous Mesoporous Mater.*, 2012, **147**, 188.
- 28 J. He, K. Ma, J. Jin, Z. Dong, J. Wang and R. Li, *Microporous Mesoporous Mater.*, 2009, **121**, 173.
- 29 A. Vinu, K. Ariga, T. Mori, T. Nakanishi, S. Hishita, D. Golberg and Y. Bando, *Adv. Mater.*, 2005, **17**, 1648.
- 30 J. H. Kaufman, S. Mein and D. D. Saperstein, *Phys. Rev. B: Condens. Matter Mater. Phys.*, 1989, **39**, 13053.
- 31 S. Dorbes, C. Pereira, M. Andrade, D. Barros, A. M. Pereira, S. L. H. Rebelo, J. P. Araújo, A. P. Pires and C. Freire, *Microporous Mesoporous Mater.*, 2012, **160**, 67.
- 32 J. L. Figueiredo, M. F. R. Pereira, M. M. A. Freitas and J. J. M. Órfão, *Carbon*, 1999, **37**, 1379.
- 33 M. A. Montes-Morán, D. Suárez, J. A. Menéndez and E. Fuente, *Carbon*, 2004, **41**, 1219.
- 34 R. M. Silverstein, F. X. Webster and D. J. Kiemle, *Spectrometric identification of organic compounds*, Wiley, New York, 7th edn, 2006.
- 35 G. Socrates, *Infrared and Raman Characteristic Group Frequencies, Tables and Charts*, John Wiley & Sons Ltd., Chichester, USA, 3rd edn, 1995, p. 327.
- 36 R. Al-Oweini and H. J. El-Rassy, *J. Mol. Struct.*, 2009, **919**, 140.
- 37 R. Silva, D. Voiry, M. Chhowalla and T. Asefa, *J. Am. Chem. Soc.*, 2013, **135**, 7823.
- 38 C. He and X. Hu, *Ind. Eng. Chem. Res.*, 2011, **50**, 14070.
- 39 (a) H. Liu, Y. Zhang, R. Li, X. Sun, S. Désilets, H. Abou-Rachid, M. Jaidann and L.-S. Lussier, *Carbon*, 2010, **48**, 1498; (b) I. Shimoyama, G. Wu, T. Sekiguchi and Y. Baba, *J. Electron Spectrosc. Relat. Phenom.*, 2001, **114–116**, 841.
- 40 (a) B. An, S. Xu, L. Li, J. Tao, F. Huang and X. Geng, *J. Mater. Chem. A*, 2013, **1**, 7222; (b) W. Xiong, M. Liu, L. Gan, Y. Lv, Z. Xu, Z. Hao and L. Chen, *Colloids Surf., A*, 2012, **411**, 34; (c) T. Kwon, H. Nishihara, H. Itoi, Q.-H. Yang and T. Kyotani, *Langmuir*, 2009, **25**, 11961.
- 41 J. Han, G. Xu, B. Ding, J. Pan, H. Dou and D. R. MacFarlane, *J. Mater. Chem. A*, 2014, **2**, 5352.
- 42 (a) K. N. Wood, R. O'Hare and S. Pylypenko, *Energy Environ. Sci.*, 2014, **7**, 1212; (b) G. Lota, B. Grzyb, H. Machnikowska, J. Machnikowski and E. Franckowiak, *Chem. Phys.*, 2005, **404**, 53; (c) S. Pylypenko, A. Borisevich, K. L. More, A. R. Corpuz, T. Holme, A. A. Dameron, T. S. Olson, H. N. Dinh, T. Gennett and R. O'Hare, *Energy Environ. Sci.*, 2013, **6**, 2957.